Heredity (2013) 111, 182–188

www.nature.com/hdy

ORIGINAL ARTICLE

Antennapedia is involved in the development of thoracic legs and segmentation in the silkworm, *Bombyx mori*

P Chen[1,3], XL Tong[1,3], DD Li[1], MY Fu[1], SZ He[1], H Hu[1], ZH Xiang[1], C Lu[1] and FY Dai[1,2]

Homeotic genes, which are associated closely with body patterning of various species, specify segment identity. The *Wedge eye-spot* (*Wes*) is a new homeotic mutant located on the sixth linkage group. Homozygous *Wes*/*Wes* embryos are lethal and display a pair of antenna-like appendages under the mouthparts as well as fused thoracic segments. These mutants also exhibit a narrower eye-spot at the larval stage compared with the wild type. By positional cloning, we identified the candidate gene of the *Wes* locus, *Bombyx mori Antennapedia* (*BmAntp*). Two *BmAntp* transcripts were identified in the homozygote of the *Wes* mutant, including a normal form and an abnormal form with a 1570-bp insertion. Our data showed that the insertion element was a long interspersed nuclear element (LINE)-like transposon that destroyed the original open reading frame of *BmAntp*. Quantitative RT-PCR analysis showed that the expression levels of normal *BmAntp* transcripts were increased markedly in the *Wes* heterozygous larvae compared with the wild type. Furthermore, we performed RNAi of *BmAntp* and observed fused thoracic segments and defective thoracic legs in the developing embryos. Our results indicated that *BmAntp* is responsible for the *Wes* mutant and has an important role in determining the proper development of the thoracic segments. Our identification of a homeotic mutation in the silkworm is an important contribution to our understanding of the regulation of *Hox* genes at different levels of expression.
Heredity (2013) **111,** 182–188; doi:10.1038/hdy.2013.36; published online 8 May 2013

Keywords: *Antennapedia*; thoracic segment; transposable elements; *Bombyx mori*

INTRODUCTION

The mechanism responsible for the development of animal body plans is fascinating because of the large diversity in animal morphology. During determination of the proper segment identity, homeotic (or *Hox*) genes encoding conserved homeodomain transcription factors, have a crucial role in characteristic patterns of segments along the anterior–posterior body axis (McGinnis and Krumlauf, 1992; Hughes and Kaufman, 2002). In arthropods, changes in *Hox* gene expression domains or in their functions can lead to the diversity of segment morphology, appendage number and pattern (Carroll, 1995; Averof and Patel, 1997).

Study of the molecular mechanism underlying the formation of homologous appendage patterns in insects is required for understanding the evolution of morphological diversity (Carroll, 2000; Jockusch *et al.*, 2004). All insects have three pairs of thoracic legs, the morphology of which is thought to be determined by *Hox* genes regulating a variety of downstream target genes related to limb development, such as *Distal-less* (*Dll*), *Wingless* (*Wg*) and *Decapentaplegic* (*Dpp*) (Jockusch *et al.*, 2000; Grienenberger *et al.*, 2003; Gebelein *et al.*, 2004). In *Drosophila melanogaster*, the homeotic *Antennapedia* (*Antp*) gene is expressed in the thoracic embryonic epidermis and is required for proper development of the thorax and legs (Abbott and Kaufman, 1986; Carroll *et al.*, 1986; Wirz *et al.*, 1986). Loss-of-function mutations in the embryo result in transformation of the second and third thoracic segments toward the prothoracic segment (Wakimoto and Kaufman, 1981). Ectopic expression of the *Antp* gene leads to distinct phenotypes, such as the transformation of antennae into second legs and eye reduction (Schneuwly *et al.*, 1987; Plaza *et al.*, 2008; Prince *et al.*, 2008). Moreover, in the spider *Achaearanea tepidariorum*, a non-insect arthropod, the *Antp* gene represses the growth of legs in the first segment of the abdomen (Khadjeh *et al.*, 2012). There are reports of extensive studies, but further exploration of the particular role of the *Antp* gene underlying the development of the thorax and thoracic appendages is needed.

In the silkworm *Bombyx mori*, >30 different homeotic mutants called the E complex have been identified and most of them show anomalies in proleg development (Tazima, 1964; Banno *et al.*, 2005). The E complex was presumed to be analogous to the *D. melanogaster* bithorax complex (BX-C; Ueno *et al.*, 1992) and studies on *B. mori* BX-C genes have suggested that all of them are involved in proleg patterning (Masumoto *et al.*, 2009; Tomita and Kikuchi, 2009). However, the *Hox* genes are complex and few of these mutants have been characterized at the molecular level.

Wedge eye-spot (*Wes*) is a new homeotic mutant that was discovered during the preservation and investigation of the characteristics of silkworm resources (Dai *et al.*, 2009). Genetic analysis revealed that it is controlled by a single dominant gene and is located at 24.3 cM on the sixth linkage in the silkworm genetic linkage map. The genetic distance between *Wes* and E^{Kp}, a member of the

[1]State Key Laboratory of Silkworm Genome Biology, Southwest University, Chongqing, China and and [2]College of Biotechnology, Southwest University, Chongqing, China
[3]These authors contributed equally to this work.
Correspondence: Professor FY Dai or Professor C Lu, State Key Laboratory of Silkworm Genome Biology, Southwest University, No. 216 Tiansheng Road, Beibei, Chongqing, 400716, China.
E-mail: fydai@swu.edu.cn or lucheng@swu.edu.cn
Received 20 November 2012; revised 19 March 2013; accepted 26 March 2013; published online 8 May 2013

E complex (Banno *et al.*, 2005; Xiang *et al.*, 2008), was ~3.0 cM (Dai *et al.*, 2009). In the present study, we identified and characterized the gene responsible for the *Wes* mutant, which induces lethality in the embryonic developmental stage of homozygotes; thus, the *Wes* mutant strain is maintained as a heterozygous stock. We demonstrated that the *Wes* locus encodes the homeodomain-containing protein BmAntp, and conclude that the abnormal *BmAntp* is responsible for the *Wes* mutant. Our results suggest that the *BmAntp* gene is essential for specifying the identify of thoracic segments.

MATERIALS AND METHODS

Silkworm strains

The *Wes* strain (*Wes*/+^{Wes}) and wild-type strain *Dazao* were used as parent strains to produce F1 offspring from a single-pair cross. As there is no recombination in female silkworms, 22 progeny from a single-pair backcross between an F1 female and a *Dazao* male (BC1F) were used for the linkage analysis and 244 progeny from the cross *Dazao* female × F1 male (BC1M) were used for the recombination analysis (Figure 2e, right). The *Wes* strain +^{Wes}/+^{Wes} used as a control was generated from *Wes* (*Wes*/+^{Wes}) mutant selfing. Silkworm strains *Wes* and *Dazao* were obtained from the Silkworm Gene Bank at Southwest University (Chongqing, China). The developing embryos were incubated at 25 °C with adequate humidity, and the larvae were reared with fresh mulberry leaves at 25 °C with a photoperiod of 12 h light/12 h dark.

Scanning electron microscopy

Embryos from developing eggs, 7 days after oviposition, were dissected under a stereomicroscope (C-DSS230, Nikon Corporation, Tokyo, Japan), fixed in 2.5% glutaraldehyde and kept at 4 °C for at least 2 h. The embryos were immersed in a phosphate buffer (0.1 M, pH 7.4) three times for 15 min each, then in 1% osmic acid for 2 h and then in water three times for 15 min each. Finally, the embryos were dehydrated by passage through a graded series of ethyl alcohol (30, 50, 60, 70, 80, 90 and 100%) for 15 min in each, then immersed in 50% 2-methyl-2-propanol, 75% 2-methyl-2-propanol, 100% 2-methyl-2-propanol, 2-methyl-2-propanol:methyl cyanide = 2:1, 2-methyl-2-propanol:methyl cyanide = 1:1, for 10 min each, then stored in methyl cyanide. The embryos were coated with gold before observation under a scanning electron microscope (S-3000N, Hitachi, Tokyo, Japan).

Genomic DNA preparation

The genomic DNA of *Wes*/*Wes* was extracted from embryos dissected from developing eggs at 7 days after oviposition using DNAzol (Invitrogen, Carlsbad, CA, USA). The genomic DNA of parental strains and BC1 individuals was extracted from adults and pupae, respectively. The samples were disrupted in liquid nitrogen and suspended in 100 μg ml^{-1} proteinase K in DNA extraction buffer (pH 8.0, 10 mM Tris-HCl, 0.1 M EDTA, 0.5% SDS) at 50 °C for 5–8 h before extraction with phenol/chloroform by standard procedures. The DNA was precipitated with cold absolute ethanol and dissolved in TE buffer (pH 8.0, 10 mM Tris-HCl, 1 mM EDTA).

Positional cloning

To construct the *Wes* linkage map, simple sequence repeat (SSR) markers on chromosome 6 (Miao *et al.*, 2005; Zhan *et al.*, 2009) and newly developed markers were screened for 22 BC1F individuals. The primers for the markers are given in Table 1. The segregation patterns in 244 BC1M individuals (Supplementary data) were analyzed using JoinMap 4.0 software (Van Ooijen, 2006), with a logarithm of the odds (LOD) threshold of 4.0 and the Kosambi mapping function (Kosambi, 1944).

According to the results of the preliminary SSR mapping, the candidate genes were analyzed using the silkworm genome database SilkDB (http://silkworm.swu.edu.cn/silkdb/) (Duan *et al.*, 2010). We used the BLASTp program (http://blast.ncbi.nlm.nih.gov/Blast.cgi; Altschul *et al.*, 2005) to find the homologous and orthologous genes associated with determining segment identity during the development of other species.

Cloning of *B. mori Antp* (*BmAntp*) fragment

Total RNA was isolated from eight 7-day-old *Dazao* and eight 7-day-old *Wes*/*Wes* embryos using the MicroElute Total RNA Kit (Omega Bio-Tek, Norcross, GA, USA) according to the manufacturer's instructions. The *Wes*/*Wes* homozygotes were distinguished from others by their fused thorax and antenna-like appendages under mouthparts. Embryos were excised with a mini-homogenizer (Polytron PT1600E, Kinematica, Lucerne, Switzerland). cDNA was synthesized from total RNA samples with oligo(dT) primers and a Moloney murine leukemia virus reverse transcriptase (Promega, Madison, WI, USA) according to the manufacturer's instructions. *Bmactin 3* was used as the internal control. We designed primers P1 and P2 according to the sequence of *Antp* (GenBank accession number: KC165846) in the silkworm (Table 1). The PCR reactions used Ex Taq (Takara, Dalian, China) under the following conditions: initial denaturation at 94 °C for 4 min; 32 cycles at 94 °C for 45 s, *Tm* (57 °C and 64 °C for P1 and P2, respectively) for 1 min, 72 °C for 1 min; and a final extension at 72 °C for 10 min. The PCR products were cloned into the pMD19-T vector (Takara) and sequenced.

Quantitative RT-PCR (qRT-PCR)

Total RNA from the whole body of fifth instar larvae was isolated using TRIzol (Invitrogen) and reverse transcription was carried out as described above. Referring to the full-length cDNA sequence of *BmAntp*, we designed the gene-specific primer set *Antp*-C (common) to detect the *BmAntp* transcripts in both wild-type and *Wes* heterozygotes, and the primer set *Antp*-M (mutant) for the mutational transcript in *Wes* heterozygotes (Table 1). The eukaryotic translation initiation factor 4A (silkworm microarray probe ID sw22934) was used

Table 1 The primer sets used in this study

Object	*Primer name*	*Sense sequence (5′–3′)*	*Antisense sequence (5′–3′)*
Linkage analysis	S0609[a]	TGCCAGCCCTCGCCTAA	GCACGGAAGCTCCAACGAC
	S0611[a]	CGTGCGTGATTTGTTTTCAGTTT	TCAGTTGCGGAACGTGCTC
	S0615[a]	CAAGAGTACATTAAAGGGCAGTGC	TGTAGTTGTGACGTAGGGGCTG
	P1	GCGGGGTCGACAAACCTACA	GTAACTTCGGCCTTCGGACC
	P2	GATTCGGAAGTGTTTGTGTTG	CATGGGTATAGCGGACTGG
dsRNAi	dsBmantp	TAATACGACTCACTATAGGGGCGGGGTCGACAAACCTACA	TAATACGACTCACTATAGGGGTAACTTCGGCCTTCGGACC
	dsEGFP	GTAATACGACTCACTATAGGGGCTGTTCACCGGGGTGGTGC	GTAATACGACTCACTATAGGGTTCTCGTTGGGGTCTTTGCT
Quantitative RT-PCR	*Antp*-C	GAGACACCGTCCGTCAACAAC	CGTATTTCCGTCGCAGATTTT
	Antp-M	CAGACGCAGATGCCCCCTAT	AGAATGCCCTTGGATGAGACG
	sw22934	TTCGTACTGCTCTTCTCGT	CAAAGTTGATAGCAATTCCCT

[a]The primers reported by Miao *et al.* (2005) and Zhan *et al.* (2009).

as the internal control. A standard curve was constructed for each target gene using a series of 10-fold dilutions of the plasmid pMD19-T containing the specific fragment. Quantitative RT-PCR (qRT-PCR) experiments were performed using the StepOnePlus real-time PCR system (Applied Biosystems, Foster City, CA, USA) with a SYBR Premix EX Taq_kit (Takara), according to the manufacturer's recommended procedure. The qRT-PCR conditions were: 95 °C for 4 min, followed by 40 cycles at 95 °C for 15 s and 60 °C for 31 s, 95 °C for 15 s, 60 °C for 20 s and 95 °C for 15 s.

RNA interference (RNAi)

Double-stranded RNAs (dsRNAs) for *BmAntp* and *EGFP* were synthesized using the RiboMAX Large Scale RNA Production System-T7 (Promega) based on the PCR templates amplified by the primer set dsBmAntp and dsEGFP, respectively (Table 1) according to the manufacturer's instructions. The dsRNA precipitate was dissolved in RNase-free water and diluted to a concentration of 5 μg μl^{-1} for injection. At 2–6 h after oviposition, the eggs were punctured on the ventral side by a micromanipulator (SZX2-STL, Olympus, Tokyo, Japan) using a spiculate metal needle and the injection of dsRNA was done with a thin-walled glass capillary (G-100, Narishige, Tokyo, Japan). The injected eggs were incubated at 25 °C with adequate humidity until dissection. The mutant phenotypes were imaged digitally with a stereomicroscope.

RESULTS

Phenotypes of the *Wes* mutant

The *Wes* mutant was discovered and named by Dai *et al.* (2009) based on the shape of the eye-spot located on the first and second thoracic segment. The eye-spot of the heterozygotic larva (*Wes*/ + ^{Wes}) looks like a narrower inverted triangle compared with the wild type (Figures 1a and d), whereas the crescents and stars are normal. The homozygote *Wes*/*Wes* is embryonic lethal.

To further characterize the homozygous mutant embryos, we dissected the embryos in the late developmental stage (6–7 days after oviposition) and observed them under a scanning electron microscope. The normal embryo has three thoracic segments (T1–T3) with one pair of thoracic legs on each (Figure 1g). On the end of each thoracic leg, there is a crochet as a sign of thoracic legs (Figures 1h and i). Amazingly, in the *Wes*/*Wes* embryos, the first thoracic legs appeared under the mouthparts and were transformed

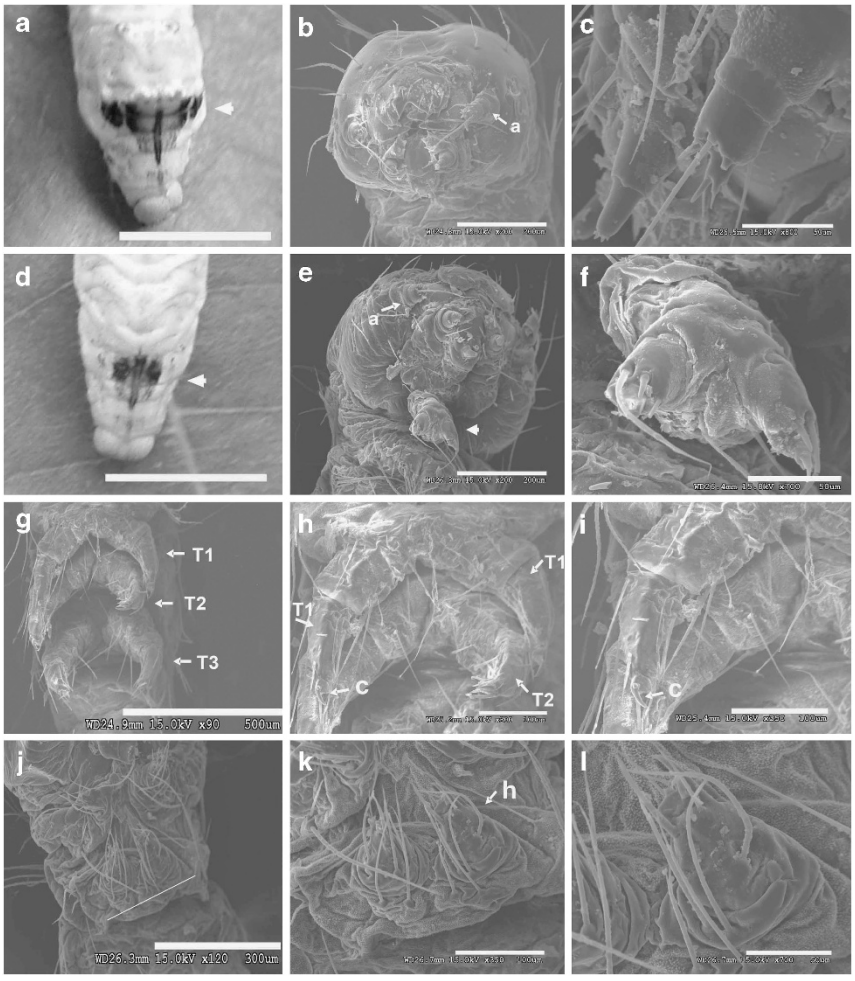

Figure 1 Phenotype and appendage morphology of the wild type and *Wes* mutant. (**a**) Eye-spot of + ^{Wes}/ + ^{Wes}. Bar = 1 cm. The arrowhead indicates the eye-spot. (**b**) Head of the *Dazao* embryo. Bar = 200 μm. (**c**) Antenna of *Dazao*. Bar = 50 μm. (**d**) Eye-spot of *Wes*/ + ^{Wes}. Bar = 1 cm. The arrowhead indicates the eye-spot. (**e**) Head of the *Wes*/*Wes* embryo. Bar = 200 μm. The arrowhead indicates the antennae-like appendages. (**f**) Enlargement of the antennae-like appendages in (**e**). Bar = 50 μm. (**g**) Thoracic segments of the *Dazao* embryo. Bar = 500 μm. (**h**) Enlargement of the same embryo in (**g**). Bar = 100 μm. (**i**) Enlargement of the thoracic leg on T1. Bar = 100 μm. (**j**) Thorax of the *Wes*/*Wes* embryo. Bar = 300 μm. (**k**) Enlargement of the same embryo in (**j**) as indicated by the the straight line. Bar = 100 μm. (**l**) Enlargement of appendage h in (**k**). Bar = 50 μm. T1, prothoracic segment; T2, mesothoracic segment; T3, metathoracic segment; a, antenna; c, crochet.

into antenna-like appendages (Figures 1e and f, compared with Figures 1b and c, respectively). The thorax of the *Wes*/*Wes* embryo appeared to be fused (Figure 1j, compared with Figure 1g), and the two remaining pairs of legs did not have the characteristics of thoracic legs, and exhibited partial homeotic transformation to antennae (Figures 1k and l, compared with Figures 1h and i, respectively).

Mapping of the *Wes* locus

To specify the candidate region responsible for the *Wes* mutant, we undertook a genetic linkage analysis using the *B. mori* SSR molecular linkage map and genome sequence. We roughly mapped the *Wes* mutant using 244 BC1M individuals with the SSR markers on the sixth linkage. The segregation ratio in BC1M individuals was 127 wild type/117 mutant, approaching 1:1. These results indicated that the *Wes* gene was localized within a 2.0-cM region linked to SSR marker S0609 (Figure 2a), which was on the nscaf2853 scaffold according to the SilkDB database (Figure 2b) (Duan *et al*, 2010).

Identification of the *Wes* candidate gene

On the basis of preliminary mapping, we biologically analyzed the available downstream genomic sequences of S0609 around a 1 Mb region (Figure 2c), and used chromosome walking. Notably, within ~300 kb downstream of the S0609 marker, we found the homeotic gene cluster that has a critical role in the specification of different anatomical segment identities. We designed primer sets based on the sequences of the *Hox* genes in *B. mori* to develop new markers between *Wes* and *Dazao*. We found that one pair of primers from *BmAntp* (P1) displayed a much larger amplification product in the *Wes* homozygote than in the wild-type *Dazao* (Figure 2d). Thereafter, when mapping with the new marker P1, we found no recombination between P1 and the *Wes* locus (Figure 2e). Comparison to the genome assembly data showed that the sequence amplified by P1 belonged to the third exon of *BmAntp*. Further, *BmAntp*, a homolog of the *Antp* gene in *D. melanogaster*, was reported to be expressed mainly in the thorax and to have an important role in identifying thorax segments (Hughes and Kaufman, 2002). Therefore, we concluded that the *BmAntp* gene was the candidate gene for the *Wes* mutant.

Sequence analysis of the candidate gene

Characterization of the genomic organization of *BmAntp* revealed that the transcription unit spanned a region of ~44 kb in the nscaf2853 scaffold on the sixth chromosome and consisted of three exons (Figure 3b). We obtained cDNA from *Wes* homozygous embryo and found two coexisting transcripts amplified by primer set P1 (Figure 3a). Cloning of these two transcripts and comparing the sequences with the wild type in *Dazao* indicated that the smaller (type 1) was the same as the normal type, whereas the larger transcript (type 2) contained a 1570 bp insertion (GenBank accession number KC165845) (Figure 3b) that destroyed the homeodomain in *BmAntp*. Interestingly, the expression level of the abnormal transcript was much higher than that of the wild type in the *Wes*/*Wes*; meanwhile, the normal transcript was expressed at a much lower level in *Wes*/*Wes* compared with the wild type (*Dazao*) (Figure 3a).

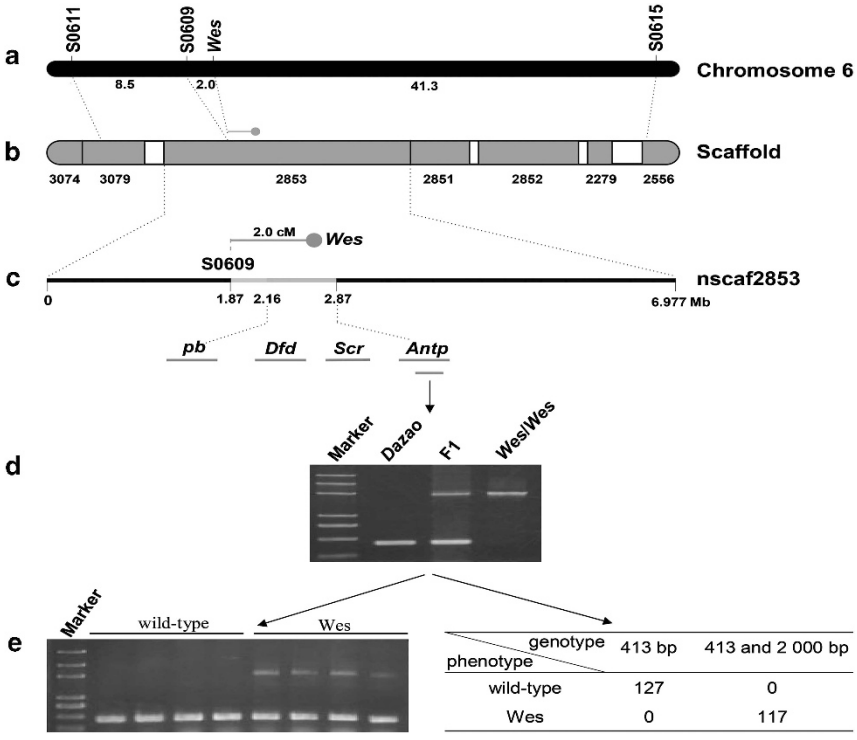

Figure 2 Mapping of *Wes* locus on *B. mori* chromosome 6. (**a**) SSR markers and genetic analysis. Three SSR markers and the *Wes* locus are shown above the map. Distances in cM are shown below the map. (**b**) Genomic scaffolds on chromosome 6. Dark gray boxes represent the assembled scaffolds and the names of the scaffolds are shown below. (**c**) Scaffold map and gene model of the nscaf2853 scaffold on chromosome 6. The SSR marker S0609 and the *Wes* locus are shown above the map. The genetic distance between S0609 and *Wes* locus is 2.0 cM. The gray and brown boxes (part of the *Hox* cluster) represent the ~1 Mb region scanning by using bioinformatics analysis and chromosome walking. Distances are shown below in Mb. *pb*, *proboscipedia*; *Dfd*, *Deformed*; *Scr*, *Sex combs reduced*; *Antp*, *Antennapedia*. (**d**) The marker P1 shows polymorphism between *Dazao* and *Wes*. The sizes of the DNA markers (up to down) are 5000, 3000, 2000, 1000, 750, 500 and 250 bp. (**d**) Mapping of the *Wes* locus using P1. Linkage analysis (left) and recombination analysis (right) by using P1. There is no recombination between P1 and the *Wes* locus.

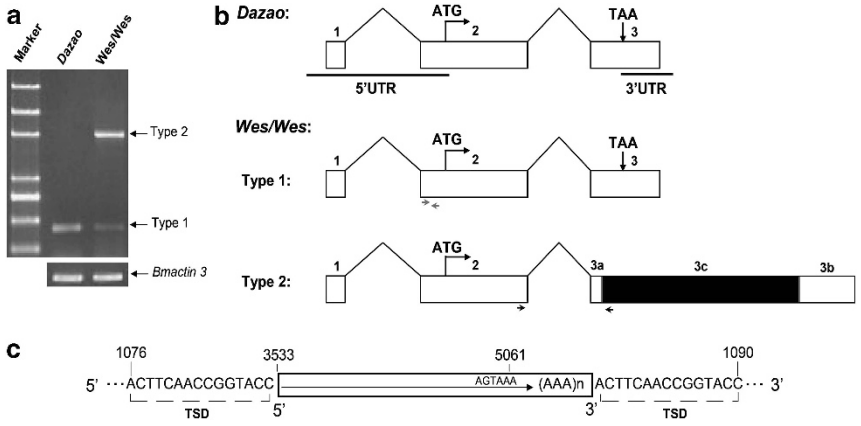

Figure 3 Schematic diagram of *BmAntp* sequences of the wild type (*Dazao*) and mutant (*Wes*/*Wes*). (**a**) *BmAntp* transcripts amplified by P1 in *Dazao* and *Wes*/*Wes*. The *Bmactin 3* was used as an internal control. (**b**) Comparison of the structure of *BmAntp* between *Dazao* and *Wes*/*Wes*. White boxes, exons; diagonal lines, introns; coarse horizontal lines, untranslated regions; black box, the insertion; gray boxes, target site duplication (TSD); gray arrows below Type 1, the primer set *Antp*-C; and black arrows below Type 2, the primer set *Antp*-M. (**c**) Diagram of a LINE-like element with a 5′ truncation insertion in exon 3 of the *BmAntp* gene. The *BmAntp* gene spans 1 551 bp and contains three exons. The 1570 bp insertion is flanked by a 15-base TSD of *BmAntp* cDNA sequence (nucleotides 1 076–1 090). Nucleotides 3 533–5061 represent the BMC1 element.

To characterize the insertion, the abnormal 1570 bp fragment containing a 29-nucleotide tract of A residues was analyzed with the BLASTN program at the National Center for Biotechnology Information. Based on BLAST results, we found that the inserted sequence was similar to a long interspersed nuclear element (LINE)-like element, BMC1, a non-LTR retrotransposon on the W chromosome of the silkworm (Abe *et al.*, 1998). The level of identity was 93% between the insertion and the 3′ end of the BMC1 as estimated by BLASTN (Zhang *et al.*, 2000). In addition, we found a duplication of 15 nucleotides as the inserted target site in *BmAntp* from nucleotides 1076 to 1090 of its cDNA sequence (Figure 3c). Consequently, the insertional event in the *Wes* mutant was consistent with the hallmarks of the retrotransposition process, including 5′ truncations, the presence of an oligo(dA)-rich tail at the 3′ end and target site duplications of 2–20 bp in length (Cordaux and Batzer, 2009).

Expression level of the *BmAntp* gene

To assess the relationship between the mutant phenotype (wedge eye-spot) and the *BmAntp* mutated state (heterozygotes), we used qRT-PCR analysis to quantify *BmAntp* levels using cDNA prepared from the whole body of fifth instar larvae. The amplified sequences of primer set *Antp*-C were shared by the two types of *BmAntp* cDNA, whereas the primer set *Antp*-M was only for the mutated *BmAntp* transcript (Figure 3). Interestingly, the result of the qRT-PCR showed that the expression level of *Antp*-C in the *Wes* mutant ($Wes/+^{Wes}$) was markedly higher than that in the wild type ($+^{Wes}/+^{Wes}$). Considering the expression level of *Antp*-C is hundreds of times higher than that of *Antp*-M in the heterozygotes, the elevated *Antp*-C expression levels in the mutant (heterozygotes) should be due to the overexpression of wild-type *Antp* (Figure 4).

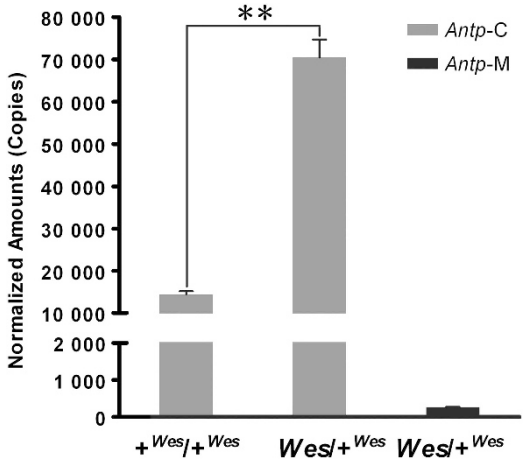

Figure 4 Quantitative analysis of *BmAntp* in $+^{Wes}/+^{Wes}$ and $Wes/+^{Wes}$ larvae. The bars indicate mean ± s.d. ($n=3$). $^{**}P<0.01$, Student's *t*-test.

Table 2 Phenotypic analysis of *BmAntp* RNAi experiment

Injection	*dsRNA concentration* ($\mu g\,\mu l^{-1}$)	*No. of embryos injected*	*No. developed embryos*	
			Normal	*BmAntp* phenotype
ddH_2O[a]		515	272	0
dsEGFP	5.0	526	169	0
dsBmAntp	5.0	857	143	36 (20.11%)

[a]Doubly distilled water.

Functional validation, RNAi of *BmAntp*

The *B. mori* larval thorax is composed of prothoracic, mesothoracic and metathoracic segments, and there is a pair of thoracic legs on each segment. The *Wes* homozygote has a deformed thorax. To validate whether a decrease of the level of *BmAntp* type 1 (wild type) mRNA is largely responsible for determining the thoracic patterning of *B. mori*, we synthesized dsRNA and injected it into eggs at 2–6 h after oviposition to suppress the expression of the *BmAntp* gene in the wild type (*Dazao*). We observed that very few eggs hatched successfully after the injection of dsBmAntp into eggs. By contrast, most of the eggs injected with doubly distilled water (ddH_2O) and dsEGFP under the same conditions (control samples) hatched after incubation. In the *BmAntp* dsRNA-treated group, a few embryos survived until the late embryonic stage and 20.11% of these exhibited morphological alteration (Table 2). Some of them showed fused

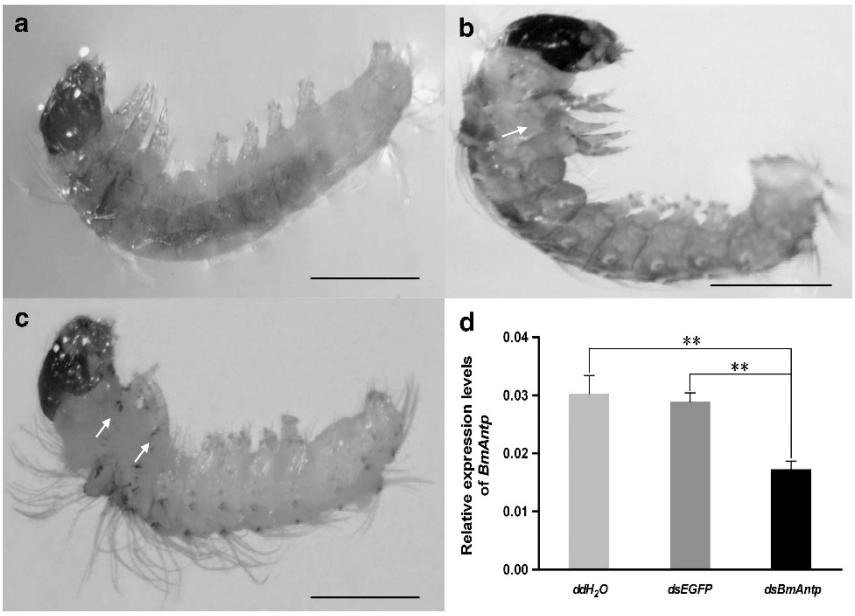

Figure 5 Effect of RNAi on *BmAntp*. (**a**) Wild type (*Dazao*) embryo injected with doubly distilled water (ddH_2O). Bar = 0.5 mm. (**b** and **c**) RNAi effects on identities of thoracic segments in embryos. After injection of dsBmAntp into the embryo, thoracic segments fused and thoracic legs were reduced partly. Bar = 0.5 mm. (**d**) Expression levels of *BmAntp* in the embryo injecting ddH_2O, dsEGFP and dsBmAntp. ddH_2O and dsEGFP-injected controls are shown for comparison. The bars indicate mean ± s.d. $^{**}P<0.01$, Student's *t*-test.

thoracic segments and the lack of a mesothoracic leg (Figure 5b), whereas others exhibited three reduced thoracic legs on one side, only remaining visible vestiges (Figure 5c). qRT-PCR revealed that the expression of *BmAntp* in the morphologically changed individuals injected with *BmAntp* dsRNA was significantly lower compared with that in the controls (Figure 5d).

DISCUSSION

Wes is a newly discovered mutant located on the sixth linkage that exhibits wedge eye-spots in the larvae and causes homeotic changes and lethality in homozygous embryos. These characteristics of *Wes* mutant provide excellent subjects for studying the developmental effects of mutant genes. An attractive strategy for identifying the gene corresponding to dramatic variations is positional cloning using *B. mori* genome information. Here, on the basis of our data, we confirmed that variations of *BmAntp* were responsible for the *Wes* phenotype.

In insects, the *Antp* gene is expressed mainly in the thorax and is associated with development of the thoracic legs (Hughes and Kaufman, 2002). Earlier studies in the beetle *Tribolium castaneum* showed that mutations in *ptl*, the *Antp* homolog, cause the transformation of the three pairs of thoracic legs to antennae (Beeman *et al.*, 1989). Similarly, loss-of-function mutations in *Antp* in *D. melanogaster* produced a homeotic transformation from the meso- and metathorax to prothorax (Wakimoto and Kaufman, 1981), and *Antp* is required for leg identity (Emerald and Cohen, 2004). In insects, the *Antp* gene is highly conserved in its morphological homeotic function, specifying segment identity. In a non-insect arthropod, the spider *A. tepidariorum*, the *Antp* gene represses the development of legs in the first segment of the abdomen (Khadjeh *et al.*, 2012). Our data showed that homozygous mutation in *BmAntp* produced the fused thorax and antennae-like appendages between the head and the thorax (Figure 1). *BmAntp* RNAi leads to fused thoracic segments and defects in the development of thoracic legs (Figure 5). Given that *Wes* homozygotes and *BmAntp*-dsRNAi embryos displayed similar mutant phenotypes, these should be owing to the loss-of-function of *BmAntp*. Our results show that *BmAntp* has an important role in thoracic segmentation. Considering the reduced thoracic legs in *BmAntp*-dsRNAi embryos and antennae-like appendages in the *Wes* homozygotes, we speculate that *BmAntp* is required for both development and identity of thoracic leg in *B. mori*.

Notably, qRT-PCR analysis revealed that the expression level of wild-type *BmAntp* gene was increased markedly in the heterozygous larvae compared with the wild type (Figure 4). This observation could reflect the fact that a negative feedback loop mechanism for *Antp* regulation has been disrupted with the disruption of a functional Antp protein. However, given that we do not know the protein level of BmAntp in the mutated state (heterozygotes), whether the mutant phenotype is owing to the BmAntp overexpression state still needs further research. Subsequently, the overexpression state of *BmAntp* mRNA in heterozygotes raises the question of why heterozygotic embryos do not show any mutant phenotype. One possibility is that the negative feedback loop has not worked in the early embryonic stage, because the thoracic legs are developing as early as ~48 h after oviposition. Another possibility is that the amount of BmAntp protein is not sufficient to cause visible developmental defects at this stage.

A previous study reported that *BmAntp* lacked the homeodomain and its downstream region in the *B. mori Nc* mutant, showing homeotic changes of prothoracic legs into antennae and compression between the prothoracic and mesothoracic segments (Nagata *et al.*, 1996). However, the transformations in *Wes* homozygotes, such as the appendages under the mouthparts (Figure 1e) and the fused thoracic segments (Figure 1j) are different, to some extent, from that in *Nc* homozygotes. Why does mutation of the same gene produce different extents of homeotic transformation? Most likely, the normal transcript in the *Wes* strain is still present, even at a very low level, but not in the *Nc* mutant. As in the previous reports that transposable element insertions in exons can function as new introns and be spliced out from pre-mRNA (Giroux *et al.*, 1994), here, we suppose

that two different *Antp* transcripts in a *Wes*/*Wes* homozygote mutant may also be due to the alternative splicing. As discussed above, an alternative explanation is that the abnormal transcript might simultaneously encode a new protein. Given that the speculative aberrant protein does not encode the homeodomain, resulting in inability to bind original target genes of *BmAntp*, we tend to favor the earlier explanation for the difference of phenotype between *Wes* and *Nc* mutants. In summary, our data imply that precise expression of the *Antp* gene is required for organization of thoracic segments.

Although *Hox* genes have been shown to regulate many downstream genes, only a limited number of *Hox*-regulated target genes have been identified (Choo and Russell, 2011). An earlier report showed that the *Ubx* gene regulated pigmentation in the hindwings of the butterfly *Precis coenia* (Weatherbee *et al.*, 1999). In addition, an intriguing case in which Hox protein abdominal-B (abd-B) directly activated expression of the *yellow* pigmentation gene in the *D. melanogaster*, demonstrated the relevance between *Hox* genes and pigmentation genes (Jeong *et al.*, 2006). Consideration of either phenomenon should be focused on the relation between pigmentation and other *Hox* genes. As mentioned above, the *Wes* eye-spot area had become smaller compared with that in the wild type. These results give rise to the hypothesis that *BmAntp* might participate in the thoracic pigmentation directly or through regulation of its downstream target genes. On the basis of these results, our future work will concentrate on the regulation of *BmAntp* and its target genes, as well as their function in pigmentation.

DATA ARCHIVING

Sequence data have been submitted to GenBank: accession numbers KC165845–KC165846.

CONFLICT OF INTEREST

The authors declare no conflict of interest.

ACKNOWLEDGEMENTS

This work was funded by National Basic Research 973 Program of China Grant (No. 2012CB114600), Hi-Tech Research and Development 863 Program of China Grant (No. 2013AA102507), National Natural Science Foundation of China (No. 31072088, No. 30901053) and Fundamental Research Funds for the Central Universities in China (No. XDJK2009C192, No. XDJK2013A001).

Abbott MK, Kaufman TC (1986). The relationship between the functional complexity and the molecular organization of the *Antennapedia* locus of *Drosophila melanogaster*. *Genetics* **114**: 919–942.

Abe H, Ohbayashi F, Shimada T, Sugasaki T, Kawai S, Oshiki T (1998). A complete full-length non-LTR retrotransposon, BMC1, on the W chromosome of the silkworm, *Bombyx mori*. *Genes Genet Syst* **73**: 353–358.

Altschul SF, Wootton JC, Gertz EM, Agarwala R, Morgulis A, Schäffer AA *et al.* (2005). Protein database searches using compositionally adjusted substitution matrices. *FEBS J* **272**: 5101–5109.

Averof M, Patel N (1997). Crustacean appendage evolution associated with changes in Hox gene expression. *Nature* **388**: 682–686.

Banno Y, Fujii H, Kawaguchi Y, Yamamoto K, Nishikawa K (2005). *A Guide to the Silkworm Mutants: 2005 Gene Name and Gene Symbol*. Kyushu University: Fukuoka, Japan.

Beeman RW, Stuart JJ, Haas MS, Denell RE (1989). Genetic analysis of the homeotic gene complex (HOM-C) in the beetle *Tribolium castaneum*. *Dev Biol* **133**: 196–209.

Carroll SB (1995). Homeotic genes and the evolution of arthropods and chordates. *Nature* **376**: 479–485.

Carroll SB (2000). Endless forms: the evolution of gene regulation and morphological diversity. *Cell* **101**: 577–580.

Carroll SB, Laymon RA, McCutcheon MA, Riley PD, Scott MP (1986). The localization and regulation of Antennapedia protein expression in *Drosophila* embryos. *Cell* **47**: 113–122.

Choo SW, Russell S (2011). Genomic approaches to understanding Hox gene function. *Adv Genet* **76**: 55–91.

Cordaux R, Batzer MA (2009). The impact of retrotransposons on human genome evolution. *Nat Rev Genet* **10**: 691–703.

Dai FY, Tong XL, Ma Y, Chen P, Lu C, Xiang ZH (2009). Genetic analysis and gene localization of a new mutant named 'Wedge eye-spot' in the silkworm, *Bombyx mori*. *Canye Kexue* **35**: 236–240, (in Chinese with English summary).

Duan J, Li R, Cheng D, Fan W, Zha X, Cheng T *et al.* (2010). SilkDB v2.0: a platform for silkworm (*Bombyx mori*) genome biology. *Nucleic Acids Res* **38**: D453–D456.

Emerald BS, Cohen SM (2004). Spatial and temporal regulation of the homeotic selector gene *Antennapedia* is required for the establishment of leg identity in *Drosophila*. *Dev Biol* **267**: 462–472.

Gebelein B, McKay DJ, Mann RS (2004). Direct integration of Hox and segmentation gene inputs during *Drosophila* development. *Nature* **431**: 653–659.

Giroux MJ, Clancy M, Baier J, Ingham L, McCarty D, Hannah LC (1994). *De novo* synthesis of an intron by the maize transposable element Dissociation. *Proc Natl Acad Sci USA* **91**: 12150–12154.

Grienenberger A, Merabet S, Manak J, Iltis I, Fabre A, Bérenger H *et al.* (2003). TGF-β signaling acts on a Hox response element to confer specificity and diversity to Hox protein function. *Development* **130**: 5445–5455.

Hughes CL, Kaufman TC (2002). Hox genes and the evolution of the arthropod body plan. *Evol Dev* **4**: 459–499.

Jeong S, Rokas A, Carroll SB (2006). Regulation of body pigmentation by the Abdominal-B Hox protein and its gain and loss in *Drosophila* evolution. *Cell* **125**: 1387–1399.

Jockusch EL, Nulsen C, Newfeld SJ, Nagy LM (2000). Leg development in flies versus grasshoppers: differences in *dpp* expression do not lead to differences in the expression of downstream components of the leg patterning pathway. *Development* **127**: 1617–1626.

Jockusch EL, Williams TA, Nagy LM (2004). The evolution of patterning of serially homologous appendages in insects. *Dev Genes Evol* **214**: 324–338.

Khadjeh S, Turetzek N, Pechmann M, Schwager EE, Wimmer EA, Damen WG *et al.* (2012). Divergent role of the Hox gene *Antennapedia* in spiders is responsible for the convergent evolution of abdominal limb repression. *Proc Natl Acad Sci USA* **109**: 4921–4926.

Kosambi DD (1944). The estimation of map distances from recombination values. *Ann Eugenics* **12**: 172–175.

Masumoto M, Yaginuma T, Niimi T (2009). Functional analysis of *Ultrabithorax* in the silkworm, *Bombyx mori*, using RNAi. *Dev Genes Evol* **219**: 437–444.

McGinnis W, Krumlauf R (1992). Homeobox genes and axial patterning. *Cell* **68**: 283–302.

Miao XX, Xub SJ, Li MH, Li MW, Huang JH, Dai FY *et al.* (2005). Simple sequence repeat-based consensus linkage map of *Bombyx mori*. *Proc Natl Acad Sci USA* **102**: 16303–16308.

Nagata T, Suzuki Y, Ueno K, Kokubo H, Xu X, Hui C *et al.* (1996). Developmental expression of the *Bombyx Antennapedia* homologue and homeotic changes in the *Nc* mutant. *Genes Cells* **1**: 555–568.

Plaza S, Prince F, Adachi Y, Punzo C, Cribbs DL, Gehring WJ (2008). Cross-regulatory protein-protein interactions between Hox and Pax transcription factors. *Proc Natl Acad Sci USA* **105**: 13439–13444.

Prince F, Katsuyama T, Oshima Y, Plaza S, Resendez-Perez D, Berry M *et al.* (2008). The YPWM motif links *Antennapedia* to the basal transcriptional machinery. *Development* **135**: 1669–1679.

Schneuwly S, Klemenz R, Gehring WJ (1987). Redesigning the body plan of *Drosophila* by ectopic expression of the homoeotic gene *Antennapedia*. *Nature* **325**: 816–818.

Tazima Y (1964). E-group as a tool of developmental genetics. In: Tazima Y. (Ed.) *The Genetics of the Silkworm*. Logos Press: London, UK, pp 60–75.

Tomita S, Kikuchi A (2009). *Abd-B* suppresses lepidopteran proleg development in posterior abdomen. *Dev Biol* **328**: 403–409.

Ueno K, Hui CC, Fukuta M, Suzuki Y (1992). Molecular analysis of the deletion mutants in the E homeotic complex of the silkworm *Bombyx mori*. *Development* **114**: 555–563.

Van Ooijen JW (2006). Joinmap 4.0, software for the calculation of genetic maps in experimental populationsKyazma BV: Wageningen, Netherlands.

Wakimoto BT, Kaufman TC (1981). Analysis of larval segmentation in lethal genotypes associated with the Antennapedia gene complex in *Drosophila melanogaster*. *Dev Biol* **81**: 51–64.

Weatherbee SD, Nijhout HF, Grunert LW, Halder G, Galant R, Selegue J *et al.* (1999). *Ultrabithorax* function in butterfly wings and the evolution of insect wing patterns. *Curr Biol* **9**: 109–115.

Wirz J, Fessler LI, Gehring WJ (1986). Localization of the Antennapedia protein in *Drosophila* embryos and imaginal discs. *EMBO J* **5**: 3327–3334.

Xiang H, Li M, Yang F, Guo Q, Zhan S, Lin H *et al.* (2008). Fine mapping of E^{kp}-1, a locus associated with silkworm (*Bombyx mori*) proleg development. *Heredity* **100**: 533–540.

Zhan S, Huang J, Guo Q, ZhaoY Li W, Miao X *et al.* (2009). An integrated genetic linkage map for silkworms with three parental combinations and its application to the mapping of single genes and QTL. *BMC Genomics* **10**: 389.

Zhang Z, Schwartz S, Wagner L, Miller W (2000). A greedy algorithm for aligning DNA sequences. *J Comput Biol* **7**: 203–214.

Supplementary Information accompanies this paper on Heredity website (http://www.nature.com/hdy)